

## (54) Steel-Polymer Concrete Composite Bridge Deck Subjected to Sagging and Hogging Bending

Xiaoqing XU <sup>1</sup>, Yuqing LIU <sup>2</sup> and Koichi MAEKAWA <sup>3</sup>

<sup>1</sup>Member of JSCE, Dept. of Civil Eng., The University of Tokyo  
(7-3-1, Hongo, Bunkyo-ku, Tokyo 113-8654, Japan)

E-mail: xu@concrete.t.u-tokyo.ac.jp

<sup>2</sup>Professor, Dept. of Civil Eng., Tongji University  
(1239 Siping Road, Shanghai 200092, P.R. China)

E-mail: yql@tongji.edu.cn

<sup>3</sup>Fellow of JSCE, Professor, Dept. of Civil Eng., The University of Tokyo  
(7-3-1, Hongo, Bunkyo-ku, Tokyo 113-8654, Japan)

E-mail: maekawa@concrete.t.u-tokyo.ac.jp

Four specimens of composite bridge deck of different kinds of concrete were fabricated and tested under static sagging or hogging bending. Polymer modified concrete mixed with basalt fiber was used in two specimens. Cracking process, strain and displacement of the specimens were recorded over the loading history. Effect of the concrete type on the behaviors of composite decks was investigated. The test results indicates that concrete tensile property is a key factor. The cracking and ultimate loads of the specimens were estimated, and the calculation was compared with the experimental ones. The applicability of in-plane hypothesis for the proposed steel-concrete composite bridge deck was examined.

**Key Words** : steel-concrete composite bridge deck, polymer modified concrete, bending, calculation method

### 1. INTRODUCTION

Steel and concrete composite slab has been one of cost-effective solutions for bridge decks in the past few decades. This type of bridge deck requires less amount of supporting girders in construction. It is of particular application for use in a long span situation, where the use of RC slabs is not feasible. In Japan, various types of composite decks have been proposed. The behavior of the composite decks has been extensively investigated since the 1980s through experimental tests and finite element simulations<sup>1)</sup>. Korean researchers<sup>2),3)</sup> also proposed an innovative composite bridge deck system and a series of experiments were conducted to validate the effectiveness of the deck system proposed. Although many researches have been conducted, there are few design specifications for steel-concrete composite bridge decks.

As for steel and concrete composite slab used widely in the floor system, one of potential ultimate limit states is the shear bond failure with slip along the interface. Standards like EC4<sup>4)</sup> have already established the design scheme to avoid it by

evaluating the longitudinal shear strength. Researchers attempted to apply the same design philosophy to the bridge decks. However, traffic loads are much heavier. Then, the design method for steel and concrete composite deck should be carefully verified. At the same time, much limited experimental data are available for behavioral investigation of composite decks subjected to negative bending. The region of decks under negative bending such as edge cantilevers is under high risk of concrete cracking as it occurs in RC decks. Since the depth of the composite deck is usually smaller than the RC one, this risk may increase and more attentions are thought to be required. Then, composite decks under static negative bending is encompassed in this study.

In this paper, four composite deck specimens were examined under positive and negative flexure. Two of them apply for polymer modified concrete, which is expected to have high durability. Failure processes of the specimens were recorded and attention is addressed to differences in structural behaviors. The experimental results are mainly used for upgrading codes for designing composite decks with a wide

variety of concrete composites in future as well.

## 2. EXPERIMENT PROGRAM

Totally, four composite deck specimens having different kinds of concrete were cast and two kinds of static bending test were performed as summarized in **Table 1**, where the characters “P” and “N” stand for positive and negative flexure, respectively. “PMC” stands for polymer modified concrete and “OC” stands for ordinary one. Two of them had configurations of single-span with two edge cantilevers and were tested under positive bending as shown in **Fig.1-2**. The rest of the specimens were half of the former ones, and were tested under negative bending as shown in **Fig.3-4**. The primary variable of interest is the kind of concrete. Structural behaviors as indicated by displacement, local strain and cracking of specimens were chiefly focused on.

**Table 1** Summary of test specimens

Bending	Specimen	Concrete
Positive	P1	PMC
	P2	OC
Negative	N1	PMC
	N2	OC

### (1) Positive bending test

**Fig.1** shows the specimens in detail. All specimens have a span of 1700mm with totally 3360mm length and 1200mm width. Under the 150mm thick concrete slab, steel plate with a thickness of 6mm was profiled to form the bottom sheeting with a 10mm high haunch. Bent bars were made from 10mm diameter rolled plain steel bars, and placed at spacing of 200mm in the transversal direction and 400mm in longitudinal one. Steel bars of 10mm diameter were placed at a spacing of 100mm in both transversal and longitudinal directions forming two layers of the steel bar mesh.

As shown in **Fig.2**, 2,000kN loading device was used to apply a concentric load on the distributive beam, which was measured with a load cell. The load was distributed to the slab through rods of 100mm diameter and steel plates of 20mm thickness, which resulted in two line loads of the same width of the specimen. Shear span of 600mm was adopted. The bearing detail consisted of rods of 100mm diameter placed between steel plates. The loading program for two specimens was similar. The first loading and the following unloading cycle with the maximum load larger the cracking load was applied under load control after the pre-loading. Then, the specimens were loaded to fail under displacement control.

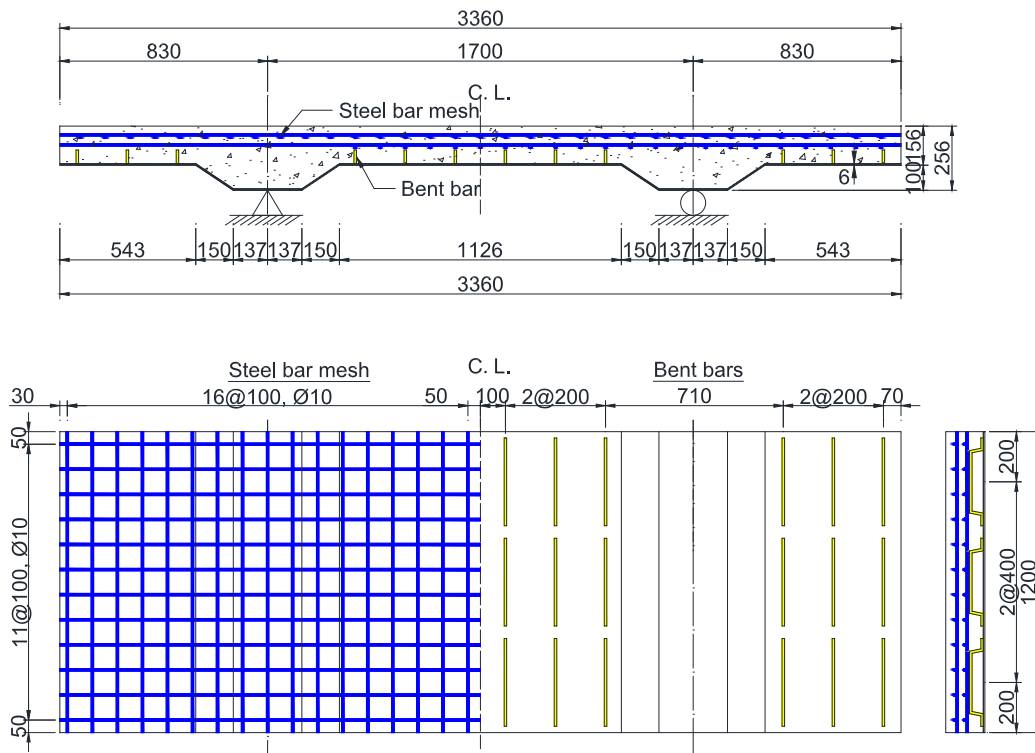


**Fig.1** Details of specimens in positive bending test

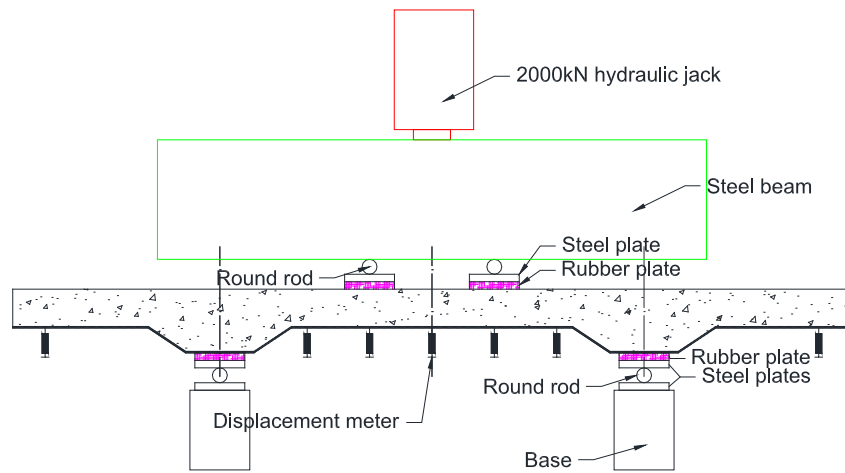


Fig.2 Test setup for positive bending test

**(2) Negative bending test**

As Fig.3 shows, the specimens under negative bending were fabricated as half of those under positive bending. Negative bending test had the similar loading program with that of positive flexure. As shown in Fig.4, 500kN loading device was used in this test to apply a point load on a steel girder, which resulted in a line load on the left side of the specimen and 700mm away from the support, while the right side of the specimen was fixed by a steel frame. Displacement control was used and the load was terminated when either the maximum stroke of the jack was reached or the displacement of specimen increased significantly.

**(3) Instrumentations**

All the specimens were similarly instrumented. Strain gauges were mounted on the steel bars and surfaces of the deck. Displacement transducers were arranged to measure vertical displacements along the specimens. Crack width and its development were also recorded by the intelligent crack observation device. The crack patterns earned were also drawn.

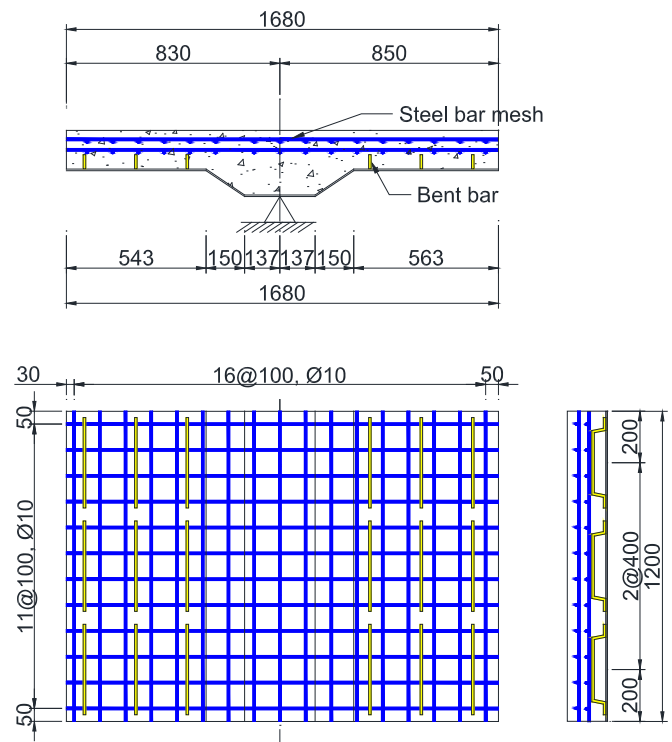


Fig.3 Details of specimens in negative bending test

**(4) Materials**

Polymer mixed concrete composite was used in two of the specimens. As listed in Table 2, this polymer composite was made by mixing with ethylene-vinyl acetate (EVA) latex and basalt fiber to obtain high durability. It was reported that sealing effect due to the polymer membranes can provide a considerable increase in water-proofness, resistance to moisture or air permeation, chemical resistance and freeze-thaw durability<sup>5)</sup>. Table 3 shows the material property test results of these concrete composites. Compared with ordinary concrete, noticeable decrease in compressive strength and Young’s modulus, and slight increase in flexural strength were obtained in PMC.

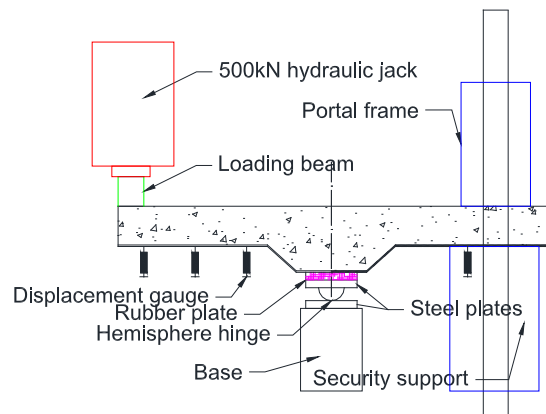


Fig.4 Test setup for negative bending test

**Table 2** Mix proportions of concrete (kg/m<sup>3</sup>)

Types	Cement	Water	Sand	Stone	Fly ash	Basalt fiber	EVA latex	W/B	P/B(wt.%)
PMC	496	156.8	646	1055	55	4	66.12	0.28	12
OC	390	192	677	890	133	-	-	-	-

P/B: polymer given as the total binder (cement, fly ash) content by mass formed.

**Table 3** Material properties of concrete

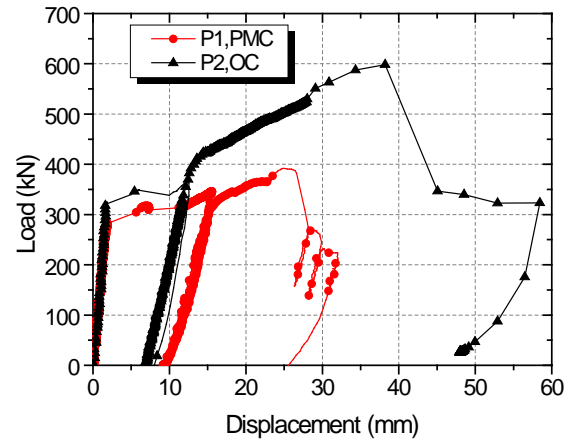
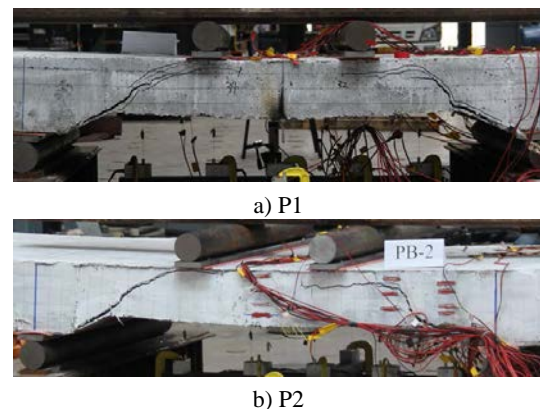
Concrete	$f_{cu}$ (MPa)	$f_{t,f}$ (MPa)	$E_c$ (GPa)
PMC	41.5	6.1	23.9
OC	51.1	5.5	29.1

### 3. EXPERIMENT RESULTS

#### (1) Positive bending

The load-displacement curves of P1 and P2 specimens with different kinds of concrete are compared as shown in **Fig.5**. The curves have a sudden decrease in stiffness after the linear elastic zone up to about 300kN. After the linearity, visible shear cracks appeared in the webs. The cracking loads for two specimens were similar. Then, both specimens underwent post-cracking inelastic deformation. The load capacity of P2 specimen was about 1.5times of that of P1. The displacement of P2 at the ultimate load was 38.2mm, while P1 was 26.1mm. It implies the higher ductility of P2, which consumed more energy than P1 before failure. As the concrete type was only the difference of two specimens and their cracking loads were similar, it can be concluded that the tensile fracture energy is the major factor on ductility. It shows that two kinds of concrete may have much different fracture energy even though they have the similar fracture strength.

**Fig.6** indicates the failure modes of the test specimens. In both specimens, cracks initiated at the section where section change starts. The initial crack occurred suddenly and caused the separation between steel plate and concrete slab. Accompanying the crack propagation to the load point and their increasing width, the separated joint interface reached the bottom of haunch. Finally, the specimens failed mainly in the mode of shear compression. An arch is thought to be formed on the upper part of the major crack, which is below the line in between the load point and the support. This arch action represents the compression strut in view of strut-tie modeling. Meanwhile, the steel plate in tension works as a tension tie, which must be anchored at the extreme ends.

**Fig.5** Load-displacement curves of P1 and P2 specimens**Fig.6** Failure modes of P1 and P2 specimens

In order to show the failure process of the specimen, pointwise strains of the section across the main crack for P1 specimen were plotted against the displacement at the mid-span (**Fig.7**). Measured strains are sequentially plotted from top to bottom, as gauges were placed in the specimen, among which No.12 gauge was on the steel plate. Two distinct stages were observed before and after cracking. The first stage was characterized by the linear and synchronous increase in strain values of these strain gauges. As a result, cross-section remained plane in this stage and the beam action predominated. At the second stage, a sudden increase in the compressive strain was observed while the tensile strain almost remained unchanged. It indicates that stress in that section was redistributed and arch action came to the reality.

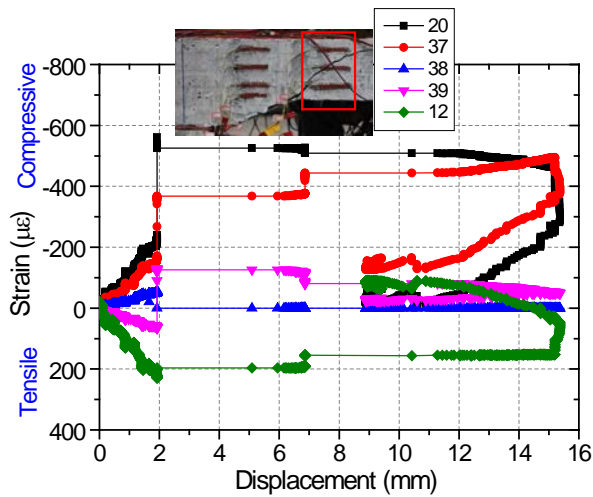


Fig.7 Strain results of P1 specimen under different displacement

**(2) Negative bending**

Fig.8 shows the load-displacement response of the specimens tested under negative bending. The responses are similar, while the loading capacity of N2 is 25% larger than that of N1. Based on visible monitoring, the cracking loads were 73kN and 82kN for N1 and N2, respectively. The behavioral difference of two specimens before cracking was smaller, while it enlarged afterwards. The load-displacement curve of N1 tends to be flat after the displacement of 30mm, while the remaining capacity tends to be increasing in that of N2. This observation is consistent with these found in P1 and P2 specimens. It implies that the post-cracking behavior of concrete is also significant for the negative bending.

As shown in Fig.9, the cracking states of N1 and N2 have been recorded and drawn with the square dotted grid of 10cm. In general, the crack spacing is approximately 15cm. However, more cracks were

observed in N1 specimen. This may be due to the fibers used in concrete. Meanwhile, the crack depth of N1 was greater. For N2, most of the cracks appeared on the fixed side of the specimen, which may be a result of asymmetric loading. In both specimens, shear cracks may be caused by the diagonal tension after the deep propagation of the several bending cracks in the slab. These cracks inclined about 45 degree and grew in the direction from the loading area or the fixed area of the slab to the haunch. This behavior is consistent with the results of fatigue tests on overhanging part of composite bridge deck reported by Kaido and Matsui<sup>6)</sup>. No visible slip occurred in either test. However, as the displacement increased with opening crack width, detached steel-to-concrete interface was observed on the bottom side of the haunch. This action seems to accompany with the shear cracks, because it only occurred on the side where shear cracks appeared.

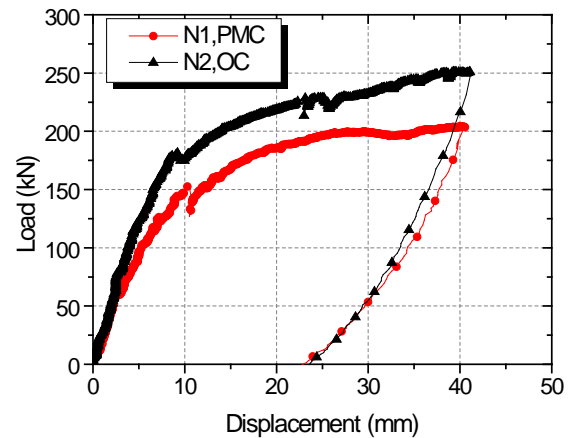


Fig.8 Load-displacement curves of N1 and N2 specimens

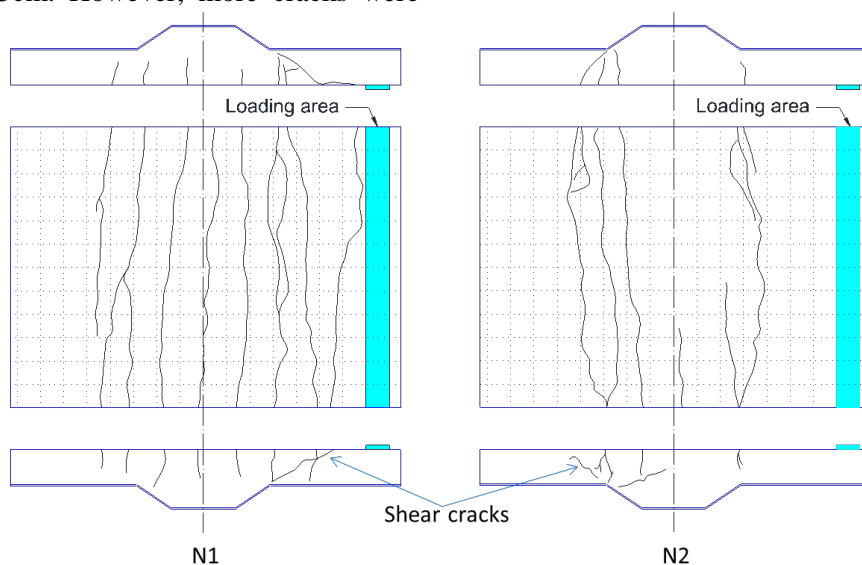
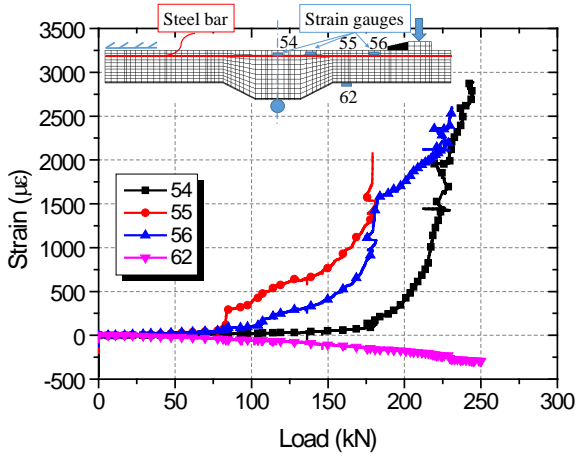


Fig.9 Cracking modes of N1 and N2 specimens

**Fig.10** shows the results of strain gauges set on the upper layer of the steel bar and the steel plate of N1. It shows that strain in the steel bar rapidly increased when the concrete was cracked, and the strain reached 2,500 micro when the specimen failed. So, the steel bar had already yielded at that time. However, in the compression region, No.62 strain gauge in the steel plate shows that steel plate was still in lower stress state. Therefore, the loading capacity of the specimen is controlled by the yield strength of steel bar.



**Fig.10** Strain results of P1 specimen under different load

### (3) Summary

The experiment results show that almost no slip occurred between steel and concrete interface under both positive and negative flexure, and the fully composite condition was guaranteed by the shear connections. Consequently, it is rational to assume that cross sections remain plane. **Table 4** summarizes the cracking and ultimate loads of the specimens. Concrete property has significant effect on the behavior of the specimen, especially the post-crack one. Concrete having larger fracture energy may result in the larger capacity and ductility. Steel plate maintains a low stress state under loading. Thus, the potential strength of the steel plate is not fully used.

**Table 4** Experiment and calculated results (kN)

	Cracking load		Ultimate load	
	Exp.	Cal.	Exp.	Cal.
P1	320	351.5	392.03	434.6
P2	365	307.3	598.40	508.1
N1	73	74.4	204.03	194.8
N2	82	71.6	251.30	215.9

## 3. COMPUTED CAPACITY

The cracking and ultimate loads of the specimens were estimated. For P1 and P2, the shear capacities were calculated while bending capacities were calculated for N1 and N2.

### (1) Under positive flexure

#### a) Cracking load

In P1 and P2 specimens, crack initiated at stress concentration point where the stress state was complicated. However, since the specimens were on a low stress state before cracking, it is reasonable to assume that steel and concrete materials were in elastic condition. Based on this assumption, the shear stress and tensile stress due to shear load and bending moment were calculated to get the principal tensile stress at the critical point.

$$\sigma_1 = \frac{\sigma_x + \sigma_y}{2} + \sqrt{\left(\frac{\sigma_x - \sigma_y}{2}\right)^2 + \tau_{xy}^2}$$

$$\sigma_x = \frac{M}{I_0} y$$

$$\tau_{xy} = \frac{V}{A_0}$$

where,  $A_0$  is area of the section which includes the area of steel bars and plates which is transformed into an equivalent concrete member;  $I_0$  is the moment inertia of the section;  $y$  is the distance from the neutral axis to the bottom tensile fiber of concrete. Stress components at the critical point were calculated and the shear stress is only 10% of the normal stress. Normal stress has greater contribution to the principle tensile stress. Then, cracking load was calculated based on the principle that shear cracking occurs at a principal tensile stress equal to concrete's tensile strength.

$$\sigma_1 = f_t$$

#### b) Ultimate load

Haunch is one of the main characteristics of the composite decks tested. For reinforcement concrete member, it is believed that the ultimate shear strength of the haunched member is a function of the haunched angle because of the inclination of the tensile resultants due to the haunch. As shown in **Fig.11**, the tensile force is inclined and introduces component transverse to the axis of the member. Then, the shear strength of the specimen is equal to

$$V_{huanch ed} = V_c - T \sin \theta' = V_c - T' \tan \theta'$$

Since,  $T' = M/Z$  and  $M = V_{huanch ed} L$ , then

$$V_{huanch ed} = V_c - \frac{V_{huanch ed} L}{Z} \tan \theta'$$

where,  $V_{huanch ed}$  is concrete shear strength for haunched slab

$V_c$  is concrete shear strength for prismatic slab with the same effective depth with the critical section

$T$  is the tension force in steel plate

$\theta$  is angle of the slope of haunch from horizontal

$\theta'$  is angle of the slope of  $T$  from horizontal

$T'$  is the vertical component of  $T$  which contributes to the external shear force

$Z$  is the level arm of the section, and  $Z = 0.8H$  was assumed

$H$  is the height of the section

$L$  is the distance between the support and the critical section

In the above equation, instead of the original geometrical angle of haunch from horizontal, the angle of steel plate from horizontal at the ultimate load was used as  $\theta'$ , which is smaller than original one due to the separation between steel plate and concrete slab as shown in Fig.6. Then,  $V_c$  was calculated according to the procedure given in the JSCE standard<sup>7)</sup> and steel plate was assumed as steel bars. Finally, the ultimate load was calculated as

$$V_u = 2V_{huanched}$$

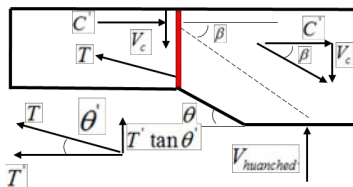


Fig.11 Forces at the critical section in decks with haunch

## (2) Under negative flexure

### a) Cracking load

When the tensile stress exceeds the concrete tensile strength, cracks form. The device of the transformed section was used. Then,

$$\sigma_x = \frac{M}{I_0} y$$

The cracking load can be calculated from the bending moment as

$$V_{cr} = 2 \times \frac{M}{L}$$

### b) Ultimate load

The main assumptions for ultimate load calculation are as follows: (1) the tensile strength of concrete is neglected; (2) steel plate and concrete slab are completely composited; (3) the effective area of the structural steel member is stressed to its design yield strength in tension or compression; and (4) the neutral axis lies on the interface between concrete slab and steel plate, and steel plate resists a compressive stress of constant over the whole depth of the steel plate. Fig.12 shows the section of the

deck. Then, ultimate load can be obtained through the moment strength per unit width of the slab calculated as

$$M_u = A_{s1} f_{y,r} \left( H - \frac{t_s}{2} - y_1 \right) + A_{s2} f_{y,r} \left( H - \frac{t_s}{2} - y_2 \right)$$

where  $A_{s1}$ ,  $A_{s2}$  are areas of each reinforcing bar layer;  $f_{y,r}$  is yield stress of reinforcing bar;  $t_s$  is thickness of steel plate;  $y_1$ ,  $y_2$  are the distances from center of steel bar to extreme tension fiber.

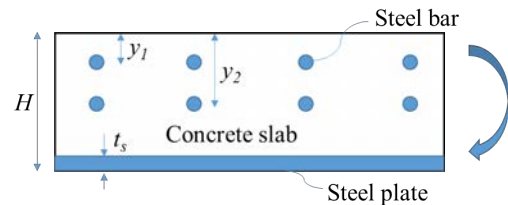


Fig.12 Calculation section of the specimen

## (3) Summary

Table 4 summarizes calculated results. For P1 and P2, the calculation results for cracking loads are close to the experimental results. However, in view of larger shear stress due to the discontinuity in geometry in specimens, the cracking load may be overestimated by those simple equations. Cracking load of P1 was calculated to be higher than that of P2. Because concrete slab has lower stress in P1 due to lower elastic modulus of PMC. However, in reality, due to the uncertainty of the construction quality, the experimental results show the opposite results.

The calculation results for shear capacities of P1 and P2 specimens are acceptable. In the calculation, steel plate is equivalent to steel bars and can increase the nominal steel ratio of the deck. Actually, in reinforced concrete member, the shear force resisted by the steel bar through dowel action is usually small. Because the steel bars are supported by the thin concrete layer below. And the bearing pressure often results in concrete splitting along the tension reinforcement. In the specimens P1 and P2, as shown in Fig.6 the similar phenomenon was observed. The folded steel plate working as a tie was straightened and deformed. Meanwhile, it bore the pressure induced by the concrete slab above. However, the steel plate was not supported. This led to large separation between steel plate and the concrete slab, and reduced the dowel action and permitted the diagonal crack to widen. Therefore, smaller shear force was resisted by steel plate, which means that steel plate can only partially be equivalent to steel bars when considering the shear strength of the composite deck.

For N1 and N2 specimens, the predicted cracking loads were accurate. Meanwhile, the predicted

ultimate loads were smaller than the experiment results. As large strains in steel bars was observed, it is possible that strain hardening occurred after yielding. In general, the assumptions for calculating specimens under negative bending are almost acceptable.

Comparing the difference between ultimate loads of specimens of different kinds of concrete, experiment results have greater value than calculated ones. Experimental uncertainty can be one of the causes. Beyond that, it is thought to be a reason that the difference in the fracture energy of concrete was not considered in calculation. It is observed that polymer modified concrete used in this study has much smaller tensile fracture energy than ordinary concrete. However, in calculation of ultimate loads of specimens under positive and negative flexure, only concrete compressive strength and yielding strength of steel are considered as the control factor respectively.

## 6. CONCLUSIONS

Four specimens of steel-concrete composite bridge decks using normal and polymer mixed concrete were fabricated and tested under static sagging and hogging bending. The cracking and ultimate loads of the specimens were focused on. The calculation capacity was compared with the experimental ones. The following conclusions are earned:

1) Through calculation, for decks under sagging bending polymer modified concrete can increase the cracking load because of lower Young's modulus and larger flexural strength.

2) Tensile properties, especially the fracture energy of concrete has the greater structural impact on the ultimate load of the bridge decks under positive flexure accompanying the detached joint interfaces of steel and concrete between shear connections.

3) But, no slip occurred and the fully composite condition can be guaranteed by the shear connections.

4) In the view of dowel action, steel plate can partially be equivalent to steel bars when considering the shear strength of the composite deck.

5) On-going design formula based upon RC members are equivalently applicable for composite decks under negative bending action.

6) Calculated results underestimated the difference between ultimate loads of specimens of different kinds of concrete because it did not take into account the effect of fracture energy of concrete.

**ACKNOWLEDGMENT:** This study was performed during the first author's academic stay at Department of Civil Engineering of The University of Tokyo in Japan with the financial support from The China Scholarship Council (CSC). The assistance is gratefully acknowledged.

## REFERENCES

- 1) Matsui, S. : Dourokyou-shouban (Bridge slabs in English), Morikita Publishing, 2007. (in Japanese)
- 2) Kim, H.Y., Jeong, Y.J. : Experimental investigation on behaviour of steel-concrete composite bridge decks with perfobond ribs, *J. Construct. Steel. Res.*, Vol. 62, pp. 463-71, 2006.
- 3) Kim, H.Y., Jeong, Y.J.: Ultimate strength of a steel-concrete composite bridge deck slab with profiled sheeting, *Eng. Struct.*, Vol. 32, No. 2, pp. 534-546, 2010.
- 4) CEN. EN 1994-1-1. Eurocode 4: Design of composite steel and concrete structures. Part 1-1: General rules and rules for buildings. Brussels; 2004.
- 5) Ohama Y. : Polymer-based admixtures, *Cement. Concr. Compos.*, Vol. 20, No. 2, pp. 189-212, 1950.
- 6) Kaido, H., Matsui, S. : Evaluation for punching shear fatigue strength of steel plate-concrete composite deck, *J. Struct. Earthquake. Eng.*, Vol. 64, No. 1, pp. 60-70, 2008. (in Japanese)
- 7) Japan Society of Civil Engineers. Standard specifications for concrete structures, 2007.